LETTERS

'Magic' nucleus ^{42}Si

J. Fridmann[1], I. Wiedenhöver[1], A. Gade[2], L. T. Baby[1], D. Bazin[2], B. A. Brown[2], C. M. Campbell[2], J. M. Cook[2], P. D. Cottle[1], E. Diffenderfer[1], D.-C. Dinca[2], T. Glasmacher[2], P. G. Hansen[2], K. W. Kemper[1], J. L. Lecouey[2], W. F. Mueller[2], H. Olliver[2], E. Rodriguez-Vieitez[3], J. R. Terry[2], J. A. Tostevin[4] & K. Yoneda[2]

Nuclear shell structures—the distribution of the quantum states of individual protons and neutrons—provide one of our most important guides for understanding the stability of atomic nuclei. Nuclei with 'magic numbers' of protons and/or neutrons (corresponding to closed shells of strongly bound nucleons) are particularly stable[1,2]. Whether the major shell closures and magic numbers change in very neutron-rich nuclei (potentially causing shape deformations) is a fundamental, and at present open, question[3,4]. A unique opportunity to study these shell effects is offered by the ^{42}Si nucleus, which has 28 neutrons—a magic number in stable nuclei—and 14 protons. This nucleus has a 12-neutron excess over the heaviest stable silicon nuclide, and has only one neutron fewer than the heaviest silicon nuclide observed so far[5]. Here we report measurements of ^{42}Si and two neighbouring nuclei using a technique involving one- and two-nucleon knockout from beams of exotic nuclei[6,7]. We present strong evidence for a well-developed proton subshell closure at $Z = 14$ (14 protons), the near degeneracy of two different ($s_{1/2}$ and $d_{3/2}$) proton orbits in the vicinity of ^{42}Si, and a nearly spherical shape for ^{42}Si.

The nuclide ^{42}Si has become the focus of particular interest in discussions of nuclear shell structure at the neutron drip line, which is the locus of the heaviest nuclides in which all the neutrons are bound to the nucleus. The nuclide ^{42}Si is only one neutron lighter than the heaviest silicon nucleus yet observed[5] and is close to the drip line, as illustrated in Fig. 1. The $N = 28$ (28 neutron) major shell closure is the lightest neutron shell closure caused by the spin-orbit force, which is responsible for all major shell closures in heavier nuclei[1,2]. However, the increasing experimental difficulty of reaching the neutron drip line with increasing proton number means that this $N = 28$ case is the only such spin-orbit shell closure that can currently be examined at the neutron drip line. In fact, it has been predicted[8–14] that this shell closure should be less well developed, or even collapse altogether, in ^{42}Si, resulting in a strongly deformed shape for this nucleus. Two recent experimental results—one a measurement[15] of the β-decay half-life of ^{42}Si and the other the determination that ^{43}Si is particle-bound[5]—have been cited in support of this view. On the other hand, ^{42}Si, with 14 protons, is expected to have a good proton subshell closure and, if the $N = 28$ major shell closure is also maintained, then ^{42}Si should have a distinctive spectroscopy characteristic of a rigidly spherical shape, like the $N = 28$ isotone ^{48}Ca or the $N = 20$ nuclide ^{34}Si (ref. 16). Shell model calculations[17] predict a situation between these two extremes: a weakly deformed shape for ^{42}Si in which the $N = 28$ shell

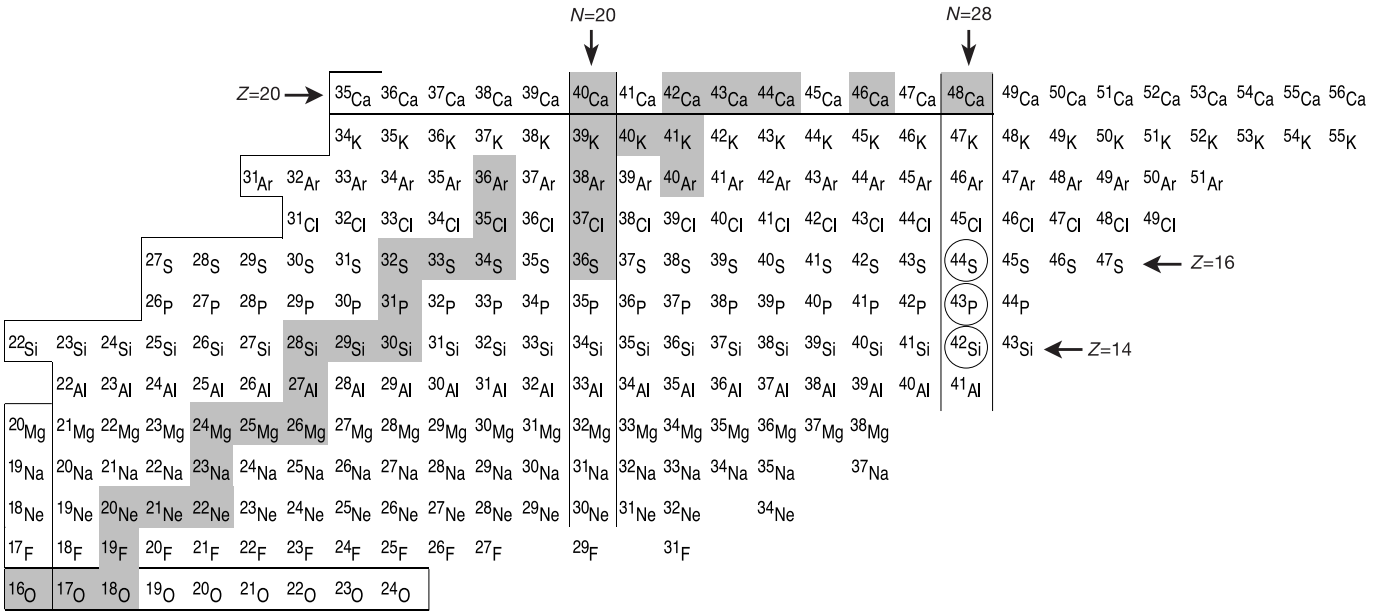

Figure 1 | A chart showing all particle-bound nuclides of the elements having $Z = 8$–20. The stable nuclides are shaded. The nuclei studied here—^{42}Si, ^{43}P and ^{44}S—are circled. *N*, number of neutrons; *Z*, number of protons.

[1]Department of Physics, Florida State University, Tallahassee, Florida 32306-4350, USA. [2]National Superconducting Cyclotron Laboratory and Department of Physics and Astronomy, Michigan State University, East Lansing, Michigan 48824-1321, USA. [3]Nuclear Science Division, Lawrence Berkeley National Laboratory, Berkeley, California 94720, USA. [4]Department of Physics, School of Electronics and Physical Sciences, University of Surrey, Guildford, Surrey GU2 7XH, UK.

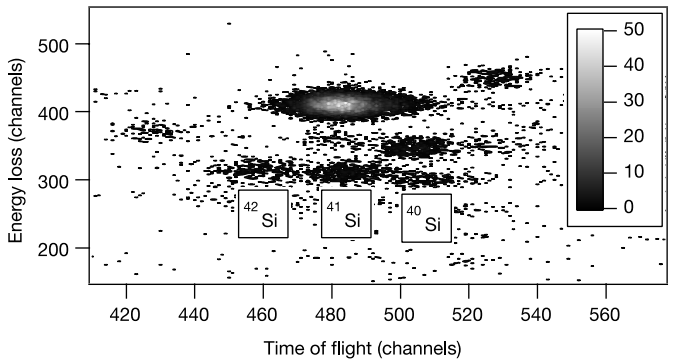

Figure 2 | Particle spectrum used to identify the two proton-knockout product ^{42}Si. Plotted are the energy loss in a plastic scintillator at the S800 spectrograph focal plane on the *y* axis, and the time of flight through the spectrograph on the *x* axis. The energy-loss signal groups ions of the same *Z* together, while the time of flight in conjunction with the magnetic rigidity selection of the spectrograph distinguishes ions according to their mass/charge ratio. The shade of grey represents the number of events detected in each bin, according to the scale displayed on the right hand side of the figure.

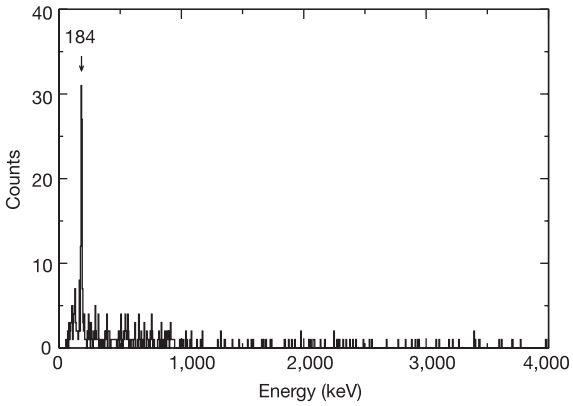

Figure 3 | The γ-ray energy spectrum in coincidence with ^{43}P residues. The γ-rays are Doppler-corrected so that the spectrum appears as in the rest frame of the residues. The γ-ray observed at 184 ± 3 keV and described in the text is labelled.

gap is narrower than in ^{48}Ca but in which the $Z = 14$ subshell closure prevents strong deformation.

In the present study, the nuclides ^{43}P and ^{42}Si were produced using respectively one- and two-proton knockout reactions with a beam of the exotic nucleus ^{44}S. In addition, a ^{46}Ar beam was used to perform spectroscopy of ^{44}S via the two-proton knockout reaction. The experiment was performed with the Coupled Cyclotron Facility (CCF) at the National Superconducting Cyclotron Laboratory (NSCL) at Michigan State University. The A1900 fragment separator[18] was used to produce the exotic beams (which had kinetic energies of 98.6 MeV per nucleon and 98.1 MeV per nucleon for ^{44}S and ^{46}Ar, respectively), the S800 spectrograph[19] to detect and identify the residues of the knockout reactions, and the SeGA array of segmented germanium detectors[20] to detect γ-rays from the residues. The knockout reactions took place in a beryllium target of thickness 375 mg cm^{-2}.

The extreme sensitivity in this experiment can be illustrated in the following way: the exotic ^{44}S and ^{46}Ar beams were produced via fragmentation reactions with a stable ^{48}Ca 'primary' beam. The primary beam current was 15 particle nanoamperes, or 3.4×10^{14} particles h^{-1}. From this, 1.5×10^{6} particles of the ^{44}S exotic beam were produced per hour. Of the three residual nuclides studied here, the one with the smallest yield was ^{42}Si, which gave 1.6 counts h^{-1}. The particle spectrum used to identify ^{42}Si is shown in Fig. 2.

The γ-ray energy spectrum obtained in coincidence with the ^{43}P residues, following one-proton removal from ^{44}S, is shown in Fig. 3. The spectrum is shown in the rest frame of the residues; that is, the γ-ray energies are Doppler corrected from the laboratory frame. A single strong γ-ray transition appears in this ^{43}P γ-ray spectrum at 184 ± 3 keV, the first γ-ray observed in this nucleus. The single-nucleon knockout reaction preferentially populates states that have a structure of a single nucleon hole in the beam nucleus[6]. The measured cross-sections for populating the two states of ^{43}P observed here—the ground state and the excited state de-excited by the 184 keV γ-ray—are large, so an interpretation of these two states as $d_{3/2}$ and $s_{1/2}$ single-proton states is justified. Their sum is 7.6(11) mb. This cross-section can be compared to theoretical cross-sections calculated for pure $d_{3/2}$ and $s_{1/2}$ single-proton states using the prescription described in refs 21 and 22. These theoretical cross-sections are 7.7 and 6.1 mb, respectively. An examination of the measured cross-section using γ-ray coincidences shows that the excited state accounts for 75 ± 15% of the cross-section. Furthermore, the 184 keV γ-ray probably connects the two states, setting the energy splitting of the two orbits.

We performed a shell model calculation of the wavefunctions of the ground state and lowest excited state in ^{43}P that provides strong evidence for the identification of the excited state with the $d_{3/2}$ proton orbit and the ground state with the $s_{1/2}$ orbit. The calculations were carried out in the model space of $(0d_{5/2},1s_{1/2},0d_{3/2})$ for protons and $(0f_{7/2},1p_{3/2},0f_{5/2},1p_{1/2})$ for neutrons with an effective interaction used in ref. 23. The computer code OXBASH[24] was used to perform the shell model calculations. The one-proton knockout cross-sections were calculated from the wavefunctions using the approach described in refs 21 and 22. According to the calculation, the state corresponding to the $d_{3/2}$ proton orbit should have 72% of the total cross-section in the present one-proton knockout reaction. The share of the cross-section measured for the excited state, 75 ± 15%, provides a strong argument for the identification of the excited state with the $d_{3/2}$ proton orbit and the ground state with the $s_{1/2}$ orbit. The near-degeneracy of these two proton orbits seen in the data (with a splitting of 184 keV) is also seen in the shell model calculation with a splitting of 1 keV. This theoretical result is consistent with the observed splitting, because shell-model calculations of this type are generally accurate to within 100–200 keV at best. The shell model fit of ref. 25 also predicted this near-degeneracy with a splitting of 100 keV.

A previous study of proton hole states populated in the potassium nuclides using the ^{X}Ca(d, ^{3}He) reaction at low energy[26] provides some perspective for the ^{43}P result. The relative energies of the $d_{3/2}$, $s_{1/2}$ and $d_{5/2}$ proton orbits extracted[16] from these data are shown in Fig. 4, as are the $Z = 8$ and $Z = 20$ major proton shell closures and the $Z = 14$ and 16 subshell closures. The energy gap between the $d_{3/2}$ and $s_{1/2}$ proton orbits decreases dramatically from more than 2 MeV in the $N = 20$ nuclide ^{39}K, where this gap forms the $Z = 16$ subshell closure, to approximately 300 keV in the $N = 28$ nuclide ^{47}K, collapsing the $Z = 16$ closure. Such shifts are observed throughout the periodic table, as demonstrated recently[27] in the tin nuclides and the $N = 82$ isotones. The separation between the $d_{5/2}$ and $s_{1/2}$ proton orbits remains large—averaging 5 MeV—throughout the K nuclides. The large energy gap between the $d_{5/2}$ proton orbit and the two higher-lying orbits forms a strong $Z = 14$ subshell closure, which is more robust than the $Z = 16$ closure. The present result shows that the $d_{3/2}$ and $s_{1/2}$ proton orbits maintain their near-degeneracy in ^{43}P. It is remarkable that the energy difference between the $d_{3/2}$ and $s_{1/2}$ proton orbits remains so stable along the $N = 28$ isotones from ^{47}K to ^{43}P (as illustrated in Fig. 4) whereas it changes so dramatically along the potassium isotopic chain.

Whereas the ^{43}P result provides strong evidence for the near-degeneracy of the $d_{3/2}$ and $s_{1/2}$ proton orbits, the cross-sections

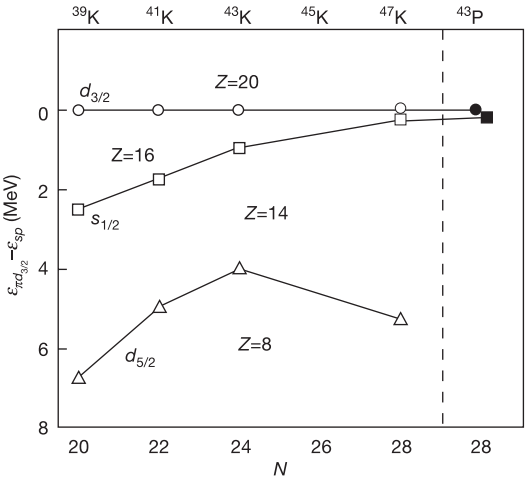

Figure 4 | Relative single proton energies. Shown are the relative energies of the $d_{5/2}$, $s_{1/2}$ and $d_{3/2}$ proton orbits in the K nuclides as extracted in ref. 14 from the data of ref. 23 (open symbols), and the relative energies of the $s_{1/2}$ and $d_{3/2}$ proton orbits in ^{43}P as determined in the present work (filled symbols). The energies are given relative to the energy of the $d_{3/2}$ proton orbit, $\varepsilon_{\pi d3/2}$, so that they are represented as the differences between the single proton energies ε_{sp} and $\varepsilon_{\pi d_{3/2}}$.

or the two-proton knockout reactions $^{44}S \rightarrow {}^{42}Si$ and $^{46}Ar \rightarrow {}^{44}S$ provide evidence that the $Z = 14$ subshell closure that exists at ^{48}Ca persists near the neutron drip line in the vicinity of ^{42}Si. The inclusive cross-sections for these reactions (0.23(2) mb for $^{46}Ar \rightarrow {}^{44}S$ and 0.12(2) mb for $^{44}S \rightarrow {}^{42}Si$) are significantly smaller than those for the other two-proton knockout reactions measured to date[7] (1.50(10) mb for $^{28}Mg \rightarrow {}^{26}Ne$; 0.76(10) mb for $^{34}Si \rightarrow {}^{32}Mg$; and 0.49(5) mb for $^{30}Mg \rightarrow {}^{28}Ne$). The cross-section for the two-proton knockout reaction depends in part on the number of valence protons in the projectile nucleus—the smaller the number of valence protons, the smaller the cross-section is expected to be[7]. If the $Z = 14$ subshell closure persists to ^{42}Si, then the number of valence protons is small in ^{46}Ar (four) and even smaller in ^{44}S (two). Therefore, the decrease in cross-section from the $^{46}Ar \rightarrow {}^{44}S$ reaction to the $^{44}S \rightarrow {}^{42}Si$ reaction is qualitative evidence for the persistence of the $Z = 14$ shell closure at $N = 28$.

We can provide a quantitative basis for this two-proton knockout discussion using a calculation that combines the shell model calculations described above—which include the $Z = 14$ subshell closure—with eikonal reaction theory. The present calculation scheme[28] is more complete than that given in ref. 7. We calculate only the dominant stripping contribution to the two-nucleon removal cross-section. As the two-proton knockout reactions are from deeply-bound single-particle states, contributions from diffraction dissociation processes are assumed to be small. The shell model calculations for the two-proton amplitudes were obtained with a truncated space of $(0f_{7/2},1p_{3/2})$ for neutrons (in order to keep feasible matrix dimensions for OXBASH[24]), but comparison with the full-space results for ^{46}Ar and ^{44}S showed that this truncation is adequate. In this calculation, the ground state of ^{42}Si is dominated (about 70%) by the closed-shell configuration of $(0d_{5/2})^6$ for protons and $(0f_{7/2})^8$ for neutrons and is therefore not well deformed, although it is not as spherical as ^{34}Si and ^{48}Ca.

The calculation yields inclusive two-proton knockout cross-sections of 0.36 mb and 0.17 mb for the $^{46}Ar \rightarrow {}^{44}S$ and $^{44}S \rightarrow {}^{42}Si$ reactions, respectively. These calculations, which include the $Z = 14$ subshell closure, reproduce the small magnitudes of the measured cross-sections (relative to those previously measured[7]); the reduction factors are similar to those of the single-proton knockout reactions. The decrease in cross-section from the $^{46}Ar \rightarrow {}^{44}S$ reaction to the $^{44}S \rightarrow {}^{42}Si$ reaction is also reproduced. A further schematic calculation in which the $Z = 14$ subshell closure is removed *ad hoc* yields cross-sections that are much larger than the data, confirming that the small observed cross-sections imply the persistence of the closure near ^{42}Si.

As pointed out in ref. 17, the persistence of the strong $Z = 14$ subshell closure in ^{42}Si will prevent strong deformation and will result in a nearly spherical shape. The present results suggest that the short lifetime of ^{42}Si, reported in ref. 15, and the existence of ^{43}Si, reported in ref. 5, must now be explained without the strong deformation assumed by the authors of those reports.

Received 13 January; accepted 24 March 2005.

1. Mayer, M. G. On closed shells in nuclei II. *Phys. Rev.* **75,** 1969–1970 (1949).
2. Haxel, O., Jensen, J. H. D. & Suess, H. E. On the "magic numbers" in nuclear structure. *Phys. Rev.* **75,** 1766 (1949).
3. Nazarewicz, W. & Casten, R. F. Physics at the Rare Isotope Accelerator (RIA): Exploring the nuclear landscape. *Nucl. Phys. A* **682,** 295c–309c (2001).
4. Warner, D. Not-so-magic numbers. *Nature* **430,** 517–519 (2004).
5. Notani, M. *et al.* New neutron-rich isotopes, ^{34}Ne, ^{37}Na and ^{43}Si, produced by fragmentation of a 64 *A* MeV ^{48}Ca beam. *Phys. Lett. B* **542,** 49–54 (2002).
6. Hansen, P. G. & Tostevin, J. A. Direct reactions with exotic nuclei. *Annu. Rev. Nucl. Part. Sci.* **53,** 219–261 (2003).
7. Bazin, D. *et al.* New direct reaction: Two-proton knockout from neutron-rich nuclei. *Phys. Rev. Lett.* **91,** 012501 (2003).
8. Werner, T. R. *et al.* Shape coexistence around $^{44}_{16}S_{28}$: The deformed N = 28 region. *Phys. Lett. B* **333,** 303–309 (1994).
9. Werner, T. R. *et al.* Ground-state properties of exotic Si, S, Ar and Ca isotopes. *Nucl. Phys. A* **597,** 327–340 (1996).
10. Terasaki, J., Flocard, H., Heenen, P.-H. & Bonche, P. Deformation of nuclei close to the two-neutron drip line in the Mg region. *Nucl. Phys. A* **621,** 706–718 (1997).
11. Lalazissis, G. A., Farhan, A. R. & Sharma, M. M. Light nuclei near neutron and proton drip lines in relativistic mean-field theory. *Nucl. Phys. A* **628,** 221–254 (1998).
12. Lalazissis, G. A., Vretenar, D., Ring, P., Stoitsov, M. & Robledo, L. M. Relativistic Hartree + Bogoliubov description of the deformed *N* = 28 region. *Phys. Rev. C* **60,** 014310 (1999).
13. Peru, S., Girod, M. & Berger, J. F. Evolution of the N = 20 and N = 28 shell closures in neutron-rich nuclei. *Eur. Phys. J. A* **9,** 35–47 (2000).
14. Rodriguez-Guzman, R., Egido, J. L. & Robledo, L. M. Quadrupole collectivity in N ≈ 28 nuclei with the angular momentum projected generator coordinate method. *Phys. Rev. C* **65,** 024304 (2002).
15. Grevy, S. *et al.* Beta-decay half-lives at the *N* = 28 shell closure. *Phys. Lett. B* **594,** 252–259 (2004).
16. Cottle, P. D. & Kemper, K. W. Persistence of the *N* = 28 shell closure in neutron-rich nuclei. *Phys. Rev. C* **58,** 3761–3762 (1998).
17. Caurier, E., Nowacki, F. & Poves, A. The N = 28 shell closure: from N = Z to the neutron drip line. *Nucl. Phys. A* **742,** 14–26 (2004).
18. Morrissey, D. J. *et al.* Commissioning the A1900 projectile fragment separator. *Nucl. Instrum. Methods Phys. Res. B* **204,** 90–96 (2003).
19. Bazin, D. *et al.* The S800 spectrograph. *Nucl. Instrum. Methods Phys. Res. B* **204,** 629–633 (2003).
20. Mueller, W. F. *et al.* Thirty-two-fold segmented germanium detectors to identify γ-rays from intermediate-energy exotic beams. *Nucl. Instrum. Methods Phys. Res. A* **466,** 492–498 (2001).
21. Tostevin, J. A. Single-nucleon knockout reactions at fragmentation beam energies. *Nucl. Phys. A* **682,** 320c–331c (2001).
22. Gade, A. *et al.* One-neutron knockout reactions on proton-rich nuclei with N = 16. *Phys. Rev. C* **69,** 034311 (2004).
23. Nummela, S. *et al.* Spectroscopy of ^{34,35}Si by β-decay: sd-fp shell gap and single-particle states. *Phys. Rev. C* **63,** 044316 (2001).
24. Brown, B.A. *et al. OXBASH for Windows* (MSU-NSCL report number 1289, National Superconducting Cyclotron Laboratory, Michigan State University, East Lansing, Michigan, 2004).
25. Duflo, J. & Zuker, A. P. The nuclear monopole Hamiltonian. *Phys. Rev. C* **59,** R2347 (1999).
26. Doll, P. *et al.* The quasihole aspect of hole strength distributions in odd potassium and calcium isotopes. *Nucl. Phys. A* **263,** 210–236 (1976).
27. Schiffer, J. P. *et al.* Is the nuclear spin-orbit interaction changing with neutron excess? *Phys. Rev. Lett.* **92,** 162501 (2004).
28. Tostevin, J. A., Podolyak, G., Brown, B. A. & Hansen, P. G. Correlated two-nucleon stripping reactions. *Phys. Rev. C* **70,** 064602 (2004).

Acknowledgements We acknowledge the support of the US National Science Foundation and the US Department of Energy.

Author Information Reprints and permissions information is available at npg.nature.com/reprintsandpermissions. The authors declare no competing financial interests. Correspondence and requests for materials should be addressed to P.D.C. (cottle@phy.fsu.edu).